Limited Live-time Measurements of Frequency Spectra

D. A. Howe, N. Ashby, D. Lirette, A. Hati, and C. Nelson

Time and Frequency Division
National Institute of Standards and Technology
Boulder, CO 80305

Abstract—**Frequency-difference-of-arrival (FDOA) can be used to monitor and track an emitter's location by observing Doppler frequency shifts of the carrier during short pulsed transmissions. This specific application needs to consider two frequency-stability levels: the short τ_{on}-average frequency measurements and the sampling time interval between measurements, denoted by τ_s. We show the advantage of using "dynamic" ThêoH for τ_{on} frequency measurements. Between τ_{on} transmissions while powered off, the emitter's reference-oscillator frequency will change due to power-start thermal variations, vibration, stress, and other frequency disturbances. If we regard long-term frequency instability as an uncertainty on an oscillator's expected or designated frequency, then the dominant error of frequency prediction is likely to be the error due to frequency drift and/or random walk FM, indicating the non-stationary behavior or disturbances. A two-sample variance is devised, called "Psi-variance," that has desirable statistical properties similar to those of the Allan variance. From this, we compute the power spectral density of frequency fluctuations, $S_y(f)$, from which phase noise, L(f), can be derived.**

I. INTRODUCTION AND SUMMARY

We characterize an oscillating signal for applications in which the oscillator itself is either only "on" or measured for short times (τ_{on}) between long, periodic or "stride" intervals (τ_s), during which the oscillator is off for τ_s - τ_{on} seconds. A statistic called Psi-deviation, $\Psi(\tau_{on},\tau_s)$, is created that estimates the frequency-prediction error from the last frequency measurement. The variance of the prediction is $\Psi^2(\tau_{on},\tau_s)$, which is a time-averaged, two-sample variance and provides desirable properties similar to the Allan variance. The application is the tracking of an emitter, transmitting only for short periods of time, by means of frequency difference of arrival (FDOA). While the emitter's oscillating signal is on and transmitting (or being measured), receivers calculate tracks based on Doppler shifts, that in turn provide a navigation solution. On a two-dimensional plane, circular error probability (CEP) due to the emitter's oscillator noise is minimized, given low enough phase noise and frequency error during the interval τ_{on}. Because τ_{on} is short and we want to optimally characterize frequency stability, we compute ThêoH [1]. Using 10 sequential segments of τ_{on}, we display each segment's ThêoH in a "waterfall" or surface plot, to characterize the oscillator's turn-on transient. Dubbed "Dynamic ThêoH", or DThêoH, it allows us to compare the

time taken by different oscillators to obtain consistent ThêoH. Oscillators having low enough cost, size, weight, and power appropriate for power cycling are OCXOs and TCXOs or oven and temperature compensated MEMs oscillators, respectively. Section II details the measurement setup and an example of DThêoH for an OCXO. Section III motivates and develops frequency prediction error $\Psi(\tau_{on},\tau_s)$. Section IV derives the relationship between Ψ-variance in the time domain and spectral density $S_y(f)$. Sections V and VI show time-domain and frequency-domain measurements, respectively, comparing an OCXO and a TCXO in limited live-time operation.

II. DYNAMIC THÊOH WHILE OSCILLATOR IS ON

We want to capture oscillator turn-on frequency stability and establish dynamic ADEV as a useful format [2]. ThêoH is preferred rather than ADEV since an oscillator is on for only a short time compared to its off-time. ThêoH is a hybrid (hence the "H") of ADEV for short-term averaging times plotted with a bias-removed version of Thêo1, called ThêoBR [3] for long-term. The Thêo portion characterizes to 75 % of a data run, whereas straight ADEV characterizes to only 20 % [1]. To illustrate, ThêoH plots are generated from measurements of oscillators powered on for a data run of only 3 s. Fig. 1 shows the measurement setup. Dynamic ThêoH is a waterfall graph where each 3 s run is parsed into ten sequential time segments, then ThêoH is computed for each segment and displayed as another waterfall plot, as shown in Fig. 2.
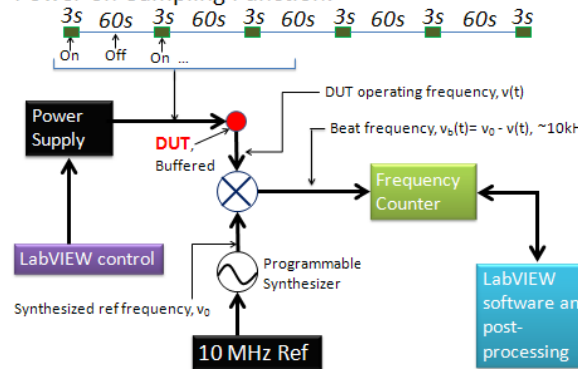

Figure 1. *The device-under-test (DUT) is a temperature-compensated or oven-controlled oscillator with quartz or MEMs*
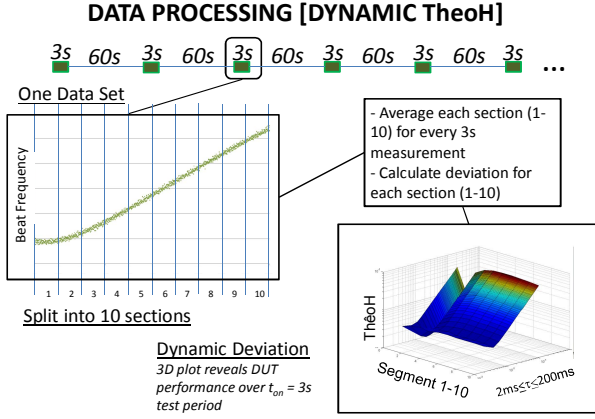
DATA PROCESSING [DYNAMIC TheoH]

Figure 2. Dynamic ThêoH plot. Surface smoothness is a general measure that the test oscillator has attained steady-state operation after having been powered on.

Such plots provide a quick assessment of how long, and to what degree, it takes an oscillator to settle down to a consistent stability after being turned on.

We will use an example in which the emitter is repeatedly turned on for τ_{on} = 3 s every τ_s = 60 s. In addition to the frequency that is traced during start-up, discussed above, an important criteria is the start-up frequency reproducibility and its characterization, described next.

III. FREQUENCY PREDICTION ERROR FOR MULTIPLES OF τ_S

We wish to estimate an oscillator's frequency at its next turn-on. While there are any number of different ways to make this estimate based on a history of actual measurements [4], we construct a two-sample frequency prediction to mimic the desirable properties of noise identification, convergence, convenience, and acceptance provided by the two-sample standard variance, better known as the Allan variance, and its square root, ADEV [5]. The two-sample, no dead-time Allan variance has widely accepted statistical properties, however, limited-live applications have substantial dead-time.

Fractional-frequency error $y_{on}(t)$ and its prediction at $y_{on}(t+\tau_s)$ is based on the reasonable assumption that (or one expects that) any given manufacturer wants $y_{on}(t+\tau_s)$ to be the same value as measured values of $y_{on}(t)$. If we write $y_{on}(t+\tau_s) = (1+\varepsilon)y_{on}(t)$, where ε is a random variable, we also expect average $\frac{1}{N}\sum_{n=1}^{N} y_{on}(t-n\tau_s)$ to be dependent on N, i.e. nonstationary, without a central limit, rendering this average of little or no practical use in the estimate of the frequency error designated as $\hat{y}_{on}(t+\tau_s)$. The efficient predictor in the presence of random walk noise is $\hat{y}_{on}(t+\tau_s) = y_{on}(t)$, the

last measured value of y_{on}. The variance of this expectation can be written as a first difference

$$\Psi^2(\tau_{on},\tau_s) = \left\langle \left[\hat{y}_{on}(t+\tau_s) - y_{on}(t)\right]^2\right\rangle, \qquad (1)$$

where $< \cdot >$ denotes an ensemble average. Like AVAR, (1) is the variance of an increment that converges in the limit.

DEFINITION: Samples of the fractional frequency-error function $y(t)$ occur at a rate f_0 having an interval $\tau_0 = \frac{1}{f_0}$ (setup shown in Fig. 1). Given a sequence of fractional frequency errors $\{y_n : n=1,...,M\}$ with a sampling period between adjacent measurements given by τ_0, we define the $m\tau_0$-average fractional-frequency deviate as

$$^{m}\overline{y}\,(t) \equiv \frac{1}{m}\sum_{j=0}^{m-1} y_{n-j},$$

where $y_n=y(t)$ with $n=t/\tau_0$ starting from a designated origin $t_0 = 0$. We also define psi-variance from the space of all possible two-sample increments as:

$$\Psi_y^2(\tau_{on},\tau_s) \equiv \left\langle \left[^{\tau_{on}}\overline{y}(t) - ^{\tau_{on}}\overline{y}(t-\tau_s)\right]^2 \right\rangle \qquad (2)$$

where $< \cdot >$ denotes an ensemble average and $^{\tau_{on}}\overline{y}(t)$ is the mean frequency over duration $\tau_{on}=m\tau_0$. Fig. 1, top, shows the sampling function associated with $\Psi^2(\tau_{on}, \tau_s)$ acting on $\{y_n\}$, where τ_{on} is called the averaging or live interval and τ_s - τ_{on} is the oscillator's dead time. Note that $\Psi^2(\tau_{on}, \tau_s)$ becomes twice the two-point standard (Allan) variance $\sigma_y^2(\tau_s)$ if $\tau_{on} = \tau_s$.

IV. RELATIONSHIP OF $S_y(f)$ TO Ψ–VARIANCE

For computing the usual power spectrum, we start with Parceval's theorem:

$$\Psi^2(\tau_{on},\tau_s) = 4\int_{\frac{1}{2\tau_s}}^{f_h} |H(f)|^2 S_y(f)df \qquad (3)$$

where $H(f)$ is the frequency-domain response of the time-domain sampling function of $\Psi^2(\tau_{on}, \tau_s)$ shown at the top of Fig. 1. $S_y(f)$ of the emitter is multiplied by the FT squared of the sampling function to obtain $|H(f)|^2$. We obtain:

$$\Psi^2(r,\tau_{on},\tau_s) = 4\int_{\frac{1}{2\tau_s}}^{f_h} \frac{S_y(f)df}{\pi^2\tau_{on}^2 f^2}\left(\sin\left(\pi\tau_{on}f\right)\sin\left(\pi r\tau_s f\right)\right)^2 \qquad (4)$$

where r = t/τ_s (starting from origin t_0) is a counting index r=1,2,3… representing the rth data run of 3 s duration.

The f-domain response function $|H(f)|^2$ is shown in Fig. 3. This response is +20dB/decade like the Allan variance for low frequencies up to the peak at $f\tau_s=\frac{1}{2}$. There is insufficient roll off above this peak, so white and flicker of phase noise types will cause the level of $\Psi^2(\tau_{on},\tau_s)$ to depend on f_h in (4).

This kind of dependence, though, is not a concern as of yet, since DUT random walk FM (and drift) are likely to dominate limited-live applications, as discussed in Section III, while white FM can occur from the measurement system at short- term.
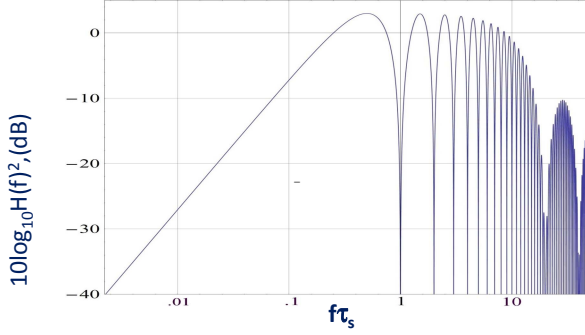
Figure 3. Frequency response $|H(f)|^2$ of $\Psi^2(\tau_{on}, \tau_s)$ in (3), $\tau_{on} = (\tau_s)/20$, $r=1$.

Table 1 compares the transform to frequency spectrum $S_y(f)$ of $\frac{1}{2}\Psi^2(\tau_{on}, \tau_s)$ and $\sigma_y^2(\tau_s)$. We use the scaling factor "1/2" in $\frac{1}{2}\Psi^2(\tau_{on}, \tau_s)$ to normalize its result to equal $\sigma_y^2(\tau_s)$ if $\tau_{on}=\tau_s$, i.e., zero dead-time. Furthermore, the zero-dead time Allan and $\frac{1}{2}\Psi^2(\tau_{on}, \tau_s)$ respond identically to white FM noise having equal frequency-spectral coefficient h_o [6]. Flicker noise is given in terms of $\sigma_y^2(\tau_s)$ to simplify the formula. The Table evidences the bias on $\sigma_y^2(\tau_s)$ due to limited-live operation of the DUT.

We now observe the intrinsic level of random walk or drift that properly characterizes the DUT as τ approaches its maximum around 2 s, using ThêoH. Since fast-frequency measurements mask or are not sensitive to DUT-based PM-noise types that would appear as "super white" FM-noise in y(t) raw data, $\frac{1}{2}\Psi^2(\tau_{on}, \tau_s)$ is never biased by this noise when compared to AVAR. Since the bias never occurs, the unbiased white-FM-transform coefficient h_0 used for $S_y(f)$ does not depend on a high-cutoff, $f_c=1/(2\tau_{on})$, as indicated in Table 1. Random walk (and drift) are slightly biased (depends on $r = \tau_s/\tau_{on}$ [7]) and the positive τ-slope is the same for $\Psi^2(\tau_{on}, \tau_s)$ and $\sigma_y^2(\tau)$. It is important to note that flicker-FM noise using dead-time AVAR (here $\Psi^2(\tau_{on}=const., \tau_s=\tau)$) will appear as white-FM noise [8].

TABLE I.   TABLE OF TRANSFORMS

Noise Type	Allan $\sigma_y^2(\tau)$	Psi Variance $\frac{1}{2}\Psi^2(\tau_{on}, \tau_s)$
White FM	$\dfrac{h_0}{2\tau}$	$\dfrac{h_0}{2\tau}$
Flicker FM	$2h_{-1}\log 2$	$\dfrac{h_{-1}}{2\tau_{on}^2}\left(\begin{array}{l} 4\tau_s\tau_{on}\tanh^{-1}\dfrac{\tau_{on}}{\tau_s} \\[2mm] +2\tau_{on}^2\ln\dfrac{\tau_s}{\tau_{on}}+ \\[2mm] (\tau_s^2+\tau_{on}^2)\ln\left(1-\dfrac{\tau_{on}^2}{\tau_s^2}\right) \end{array}\right)$
Random Walk FM	$\dfrac{2\pi^2 h_{-2}}{3}\tau$	$\dfrac{\pi^2 h_{-2}}{3}(3\tau_s-\tau_{on})$

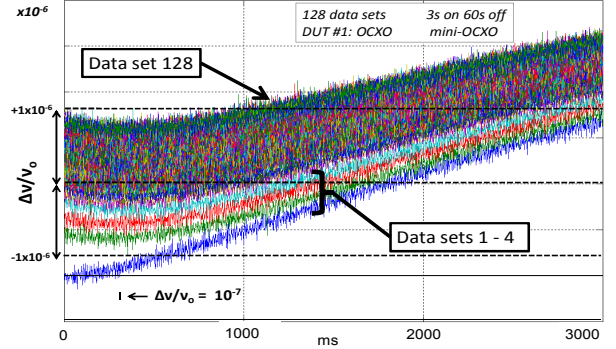Figure 4. 128 sets of raw fractional frequency measurements. Set 1 is the first series of y(t), and the oscillator is first turned on from a "cold" start. Each trace is 3 s worth of data repeating every 60 s during which the oscillator is turned off. $\nu_o = 16.384MHz$.

It remains to be seen if flicker-FM can be reliably detected by unraveling Ψ-variance to obtain AVAR. However, this distinction is usually unimportant to Doppler-relevant applications.

V.   TIME DOMAIN MEASUREMENTS OF OSCILLATORS

We use a commercial miniature OCXO and TCXO at 16.384 and 26 MHz, respectively, as DUTs for an example. Fig. 4 shows 128 raw $y(\tau_{on})$ data runs of 2 ms sampled measurements on top of each other. At the very bottom, data set #1 starts the test oscillator. One can see that the first four sets capture a larger set-to-set overall variation than the remaining 124. In real applications, the oscillators are not cold-started but are in process, so the initialization sets such as 1 to 4 can generally be ignored. We process individual runs of Fig. 4 with dynamic ThêoH as described in Section II. This is shown in Fig. 5 along with averages of ThêoH. One can see that a consistent level of stability (drift+white FM) is reached after about 60 ms. Measurements are an equispaced sequence of fast-frequency errors, y(t), and are not time-errors, x(t). Thus, measurement noise is white FM and not typified by PM noise during runs of τ_{on}. Fig. 5 shows measurement white FM in short-term, i.e., $\sigma_y(\tau_0)\propto\tau^{-1/2}$.
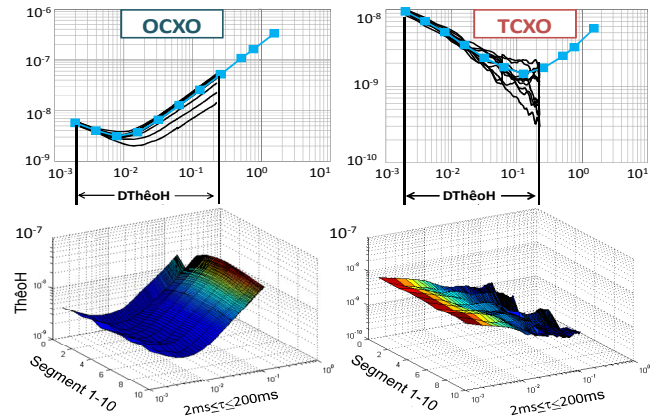

Figure 5. ThêoH deviation (top) and dynamic ThêoH (DThêoH) deviation (bottom) for the OCXO and TCXO. Note that the longest τ for DThêoH corresponds to 1/10 of the longest τ for ThêoH.
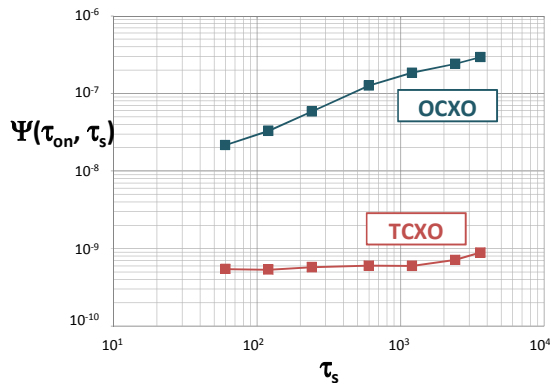
Figure 6. *Ψ-deviation for the OCXO and TCXO. The minimum averaging time is $\tau_s = 60\,s.\ \ \tau_{on} = 3\,s.$*

Figure 7. *L(f) for the OCXO and TCXO from dead-time measurements.*

With the average of each data run, $^{\tau_{on}=3s}\overline{y}(t)$, we compute $\Psi^2(\tau_{on},\ \tau_s)$ using all runs. Results are shown in Fig. 6, where we observe the level and rate of frequency reproducibility as a function of $n\tau_s$ for each time that the DUT is powered on. This level and rate may or may not limit other application-specific goals. Likewise, with a given level and rate, one may be forced to use application strategies or improve emitter reproducibility to achieve goals. Our finding is that there is no reliable method for estimating $\Psi(\tau_{on},\ \tau_s)$ from $\sigma_y(\tau)$.

VI. FREQUENCY DOMAIN MEASUREMENTS OF OSCILLATORS

Phase noise L(f) is important during limited-live Doppler tracking. L(f) is a convenient standard used to determine the error vs. range in offset-f, proportional to emitter velocity, as set by the emitter. L(f) is computed from the fast-frequency measurements obtained using Fig. 1. For a given τ_{on} data run sampled at t_0, the fractional-frequency spectrum $S_y(f)$ is obtained from the discrete FT of the series [6]:

$$Y(m\Delta f) = \frac{1}{N}\sum_{k=1}^{N} y(k\tau_0)e^{-2\pi i m\Delta fk\tau_0} \qquad (5)$$

where $\Delta f = 1/(N\tau_0)$. The one-sided spectral density of y(t) is computed by adding the squares of the real and imaginary components of Y and dividing by the RBW of the data run:

$$S_y(m\Delta f) = 2\frac{\left\{\mathrm{Re}\left[Y(m\Delta f)\right]\right\}^2 + \left\{\mathrm{Im}\left[Y(m\Delta f)\right]\right\}^2}{\Delta f} \quad (6)$$

with BW = 1 Hz and RBW = Δf. Converting to L(f), we use [6]:

$$L(m\Delta f) = \frac{1}{2}S_\phi(m\Delta f) = \frac{1}{2}\frac{v_0^2}{(m\Delta f)^2}S_y(m\Delta f) \qquad (7)$$

and obtain L(f) plotted on log-log scales in Fig 7.

In practice, the noise of each limited-live spectrum affects Doppler-track error. Averages of limited-live estimates of L(mΔf) are shown in Fig. 7 for TCXOs #1 and #2. A word of caution — L(f) derived from fast-frequency measurements in
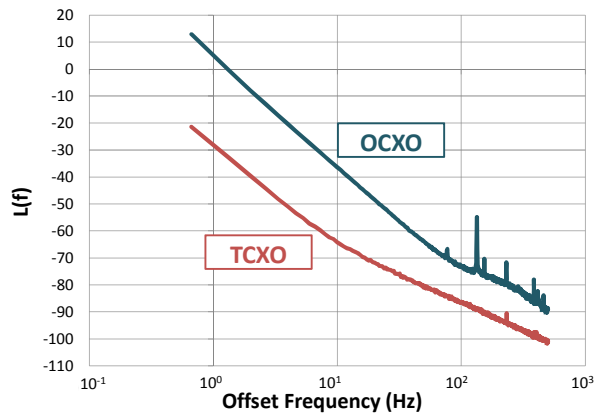
Fig. 1 will not be sensitive to white and flicker PM noise, as mentioned earlier. This is not problematic to most limited-live characterizations, since the measurement high frequency cutoff (BW) is $f_c = 1/(2\tau_0)$ and τ_0 is of the order 10^{-3} in this case. Thus, L(f) is not computed beyond f of several hundred hertz, even in the best case.

For future studies, characterization of limited-live oscillators in this paper will be used while such oscillators are subject to temperature and vibration stresses.

REFERENCES

[1] D.A. Howe, "ThêoH: a hybrid, high-confidence statistic that improves on the Allan deviation," Metrologia, IOP, UK vol. 43, pp.S322-S331, 2006.

[2] L. Galleani and P. Tavella, "Tracking Nonstationarities In Clock Noises Using the Dynamic Allan Variance," FCS/PTTI, Vancouver, BC, pp.392-396, Aug. 2005.

[3] J.A. Taylor and D.A. Howe, "Fast TheoBR: A Method for Long Data Set Stability Analysis," IEEE Trans., vol.57, no. 9, pp.2091-2094, Sept. 2009.

[4] J. Levine, "Introduction to Time and Frequency Metrology," Review of Scientific Instruments, Vol. 70, pp 2567-2596, 1999.

[5] D.W. Allan, "Statistics of Atomic Frequency Standard," IEEE Proc., 54, No. 2, pp.221-231, 1966.

[6] D.A. Howe, D.W. Allan, and J.A. Barnes, "Properties of Signal Sources and Measurement Methods," Proc. 35th Annual Symp. on Freq. Control, A1-A48, 1981. Also see NIST Technical Note 1337, editors D.B. Sullivan, D.W. Allan, D.A. Howe, and F.L. Walls, March 1990, available at http://tf.boulder.nist.gov/general/pdf/868.pdf

[7] J.A. Barnes, "Tables of Bias Functions, B₁ and B₂, for Variances Based on Finite Samples of Processes with Power Law Spectral Densities," NBS Technical Note 375, Jan. 1969.

[8] P. Lesage, "Characterization of Frequency Stability: Bias Due to the Juxtaposition of Time-Interval Measurements," *IEEE Trans. Instrum. Meas.*, Vol. IM-32, No. 1, pp.204-207, March 1983.